

## Vertical and lateral soil moisture patterns on a Mediterranean karst hillslope

Yolanda Canton<sup>1\*</sup>, Emilio Rodríguez-Caballero<sup>1,2</sup>, Sergio Contreras<sup>3</sup>, Luis Villagarcía<sup>4</sup>, Xiao-Yan Li<sup>5</sup>, Alberto Solé-Benet<sup>6</sup>, Francisco Domingo<sup>6</sup>

<sup>1</sup> Departamento de Agronomía, Escuela Superior de Ingeniería, Universidad de Almería, La Cañada de San Urbano S/N, 04120 Almería, Spain.

<sup>2</sup> Max Planck Institute for Chemistry, Multiphase Chemistry Department, Multiphase Chemistry, Mainz, Hahn-Meitner-Weg 1, 55128 Mainz, Germany. Tel.: +49-(0)6131-305-6502. E-mail: e.rodriiguez-caballer@mpic.de

<sup>3</sup> FutureWater, Paseo Alfonso XIII, 48, 30203 Cartagena, Spain. E-mail: s.contreras@futurewater.es

<sup>4</sup> Departamento de Sistemas Físicos, Químicos y Naturales, Universidad Pablo Olavide, Sevilla, Spain. E-mail: lvilsai@upo.es

<sup>5</sup> College of Resources Science & Technology, Beijing Normal University, Beijing 100875, China. E-mail: xyli@bnu.edu.cn

<sup>6</sup> Estación Experimental de Zonas Áridas, Consejo Superior de Investigaciones Científicas, La Cañada de San Urbano S/N, 04120 Almería, Spain. E-mail: albert@eeza.csic.es, poveda@eeza.csic.es

\* Corresponding author. Tel.: +34 950 01 59 59. Fax: +34 950 01 53 19. E-mail: ycanton@ual.es

**Abstract:** The need for a better understanding of factors controlling the variability of soil water content ( $\theta$ ) in space and time to adequately predict the movement of water in the soil and in the interphase soil-atmosphere is widely recognised. In this paper, we analyse how soil properties, surface cover and topography influence soil moisture ( $\theta$ ) over karstic lithology in a sub-humid Mediterranean mountain environment. For this analysis we have used 17 months of  $\theta$  measurements with a high temporal resolution from different positions on a hillslope at the main recharge area of the Campo de Dalías aquifer, in Sierra de Gádor (Almería, SE Spain). Soil properties and surface cover vary depending on the position at the hillslope, and this variability has an important effect on  $\theta$ . The higher clay content towards the lower position of the hillslope explains the increase of  $\theta$  downslope at the subsurface horizon throughout the entire period studied. In the surface horizon (0–0.1 m),  $\theta$  patterns coincide with those found at the subsurface horizon (0.1–0.35 m) during dry periods when the main control is also exerted by the higher percentage of clay that increases downslope and limits water depletion through evaporation. However, in wet periods, the wettest regime is found in the surface horizon at the upper position of the hillslope where plant cover, soil organic matter content, available water, unsaturated hydraulic conductivity ( $K_{unsat}$ ) and infiltration rates are higher than in the lower positions. The presence of rock outcrops upslope the  $\theta$  sampling area, acts as runoff sources, and subsurface flow generation between surface and subsurface horizons also may increase the differences between the upper and the lower positions of the hillslope during wet periods. Both rock and soil cracks and fissures act disconnecting surface water fluxes and reducing run-on to the lower position of the hillslope and thus they affect  $\theta$  pattern as well as groundwater recharge. Understanding how terrain attributes, ground cover and soil factors interact for controlling  $\theta$  pattern on karst hillslope is crucial to understand water fluxes in the vadose zone and dominant percolation mechanisms which also contribute to estimate groundwater recharge rates. Therefore, understanding of soil moisture dynamics provides very valuable information for designing rational strategies for the use and management of water resources, which is especially urgent in regions where groundwater supports human consume or key economic activities.

**Keywords:** Soil moisture; Soil water content; Hillslope; Soil properties; Runoff; Karstic; Mediterranean.

### INTRODUCTION

Soil moisture ( $\theta$ ) is an essential element of the water balance and it affects different linked processes: infiltration (Albertson and Montaldo, 2003; Cerdà, 1997; Rivera et al., 2014), runoff (Ceballos et al., 2002; Dehotin et al., 2015), subsurface flow (Gish et al., 2005), deep drainage (Eilers et al., 2007) and evapotranspiration (Chamizo et al., 2013; Rodríguez-Iturbe and Porporato, 2004; Tromp-van Meerveld and McDonnell, 2006) acting at different spatial and temporal scales (Canton et al., 2004; Entin et al., 2000; Martínez-Fernández and Ceballos, 2003). At the same time, all those processes exert a fundamental control on  $\theta$  patterns (Entekhabi et al., 1996; Tromp-van Meerveld and McDonnell, 2006; Western et al., 2004). In Mediterranean environments, the high spatial and temporal variability of rainfall and high incoming solar radiation, typical of these regions, are the main factor controlling the variations of  $\theta$  (Canton et al., 2004; Grayson et al., 2006; Martínez-Fernández and Ceballos, 2003; Rivera et

al., 2014; Wilson et al., 2004). Despite the fact that at coarse spatial scale factors such as rainfall and evapotranspiration constitute the main controls on  $\theta$ , at small basin and hillslope scales, the variance of  $\theta$  mainly depend on factors like soil properties, surface cover or topography (Calvo-Cases et al., 2003; Canton et al., 2001; Zhang et al., 2012; Zhao et al., 2013). In general, higher infiltration rates have been reported on coarse textured soils than on fine textured ones (Saxton et al., 1986), contributing to increase water movement into the soil. Nevertheless, it is also known that clay soils have higher  $\theta$ , because of their high water retention capacity (Jawson and Niemann, 2007). Topography and surface cover, on the other hand, control water redistribution, which also exert an important effect on  $\theta$  temporal and spatial patterns (Cammeraat, 2004; Ludwig et al., 2005). Particularly, in Mediterranean catchments, higher  $\theta$  contents are expected at the lower hillslopes positions, resulting from run-on from the upslope areas (Puigdefábregas, 2005; Yang et al., 2016). Besides this general fact, rock outcrops and physical or biological soil crusts

act as runoff sources (Canton et al., 2011; Rodríguez-Caballero et al., 2014) whereas vegetation and micro-depressions act as runoff sinks, increasing water infiltration (Mayor et al., 2008; Puigdefàbregas, 2005). Thus, general patterns of  $\theta$  on semiarid Mediterranean areas may depend on the individual effect of these factors, but they are also affected by the interactions among them (Yang et al., 2016; Zhao et al., 2013), and both, the individual effects and the interactions, vary depending on antecedent  $\theta$  conditions and rainfall properties (Rodríguez-Caballero et al., 2015).

The need for a better understanding of the complex interactions among factors that govern the spatial variability of  $\theta$  on detailed spatial scales to adequately predict the movement of water in the soil and in the interphase soil-atmosphere is widely recognised by researchers (Canton et al., 2004; Famiglietti et al., 1998; Gomez-Plaza et al., 2001; Hébrard et al., 2006; Yoo et al., 2005; Zhang et al., 2012), especially in many Mediterranean coastal areas. On these areas water demand has undergone a significant increase due to the expansion in agriculture and tourism (Benoit and Comeau, 2005). Nevertheless, the Mediterranean water regime, by itself, does not support this high demand (Castro et al., 2015), and remote carbonate karst areas, often act as recharge areas. An example is Campo de Dalías, a coastal plain in SE Spain with a highly profitable horticulture and tourist industry that result in an overexploitation of deep aquifers which are recharged by Sierra de Gador (Campra et al., 2008; Pulido-Bosch et al., 2000). Clarifying the spatial and temporal patterns of  $\theta$ , and the main factors controlling this pattern in the recharge areas, as in the case of Sierra de Gador, constitutes a key step towards estimating recharge rates and towards developing a sustainable water resource management at a basin scale. Many studies analysing  $\theta$  patterns on semiarid areas at different spatial and temporal scales (Chamizo et al., 2013; Jia et al., 2013; Koster et al., 2004; Penna et al., 2013; Rivera et al., 2014) have been conducted. However, less attention has been paid to heterogeneous and hydrologically complex karst regions, in spite of the important role that  $\theta$  plays on their structure, function and diversity (Zhang et al., 2012). In these areas, monitoring of  $\theta$  is difficult to carry out because of soils are usually shallow, rocks are frequent and discontinuously distributed. Furthermore, the numerous cracks and fissures, enhanced by carbonate dissolution, usually promote preferential water fluxes complicating  $\theta$  monitoring. Thus, the complexity of the interactions between  $\theta$  and its drivers increase in these karstic systems (Pena et al., 2013; Tokumoto et al., 2014) remaining unclear up to now (Yang et al., 2016; Zhang et al., 2012). Moreover, the knowledge of soil moisture dynamics in the vadose zone provides valuable information to understand the dominant percolation mechanism and the temporal and spatial variability of groundwater recharge (Ries et al., 2015).

In order to identify the factors controlling the vertical and lateral patterns of  $\theta$ , at the main morpho-structural domain of recharge to the deep aquifers of Campo de Dalías, the influence of soil properties, surrounding surface cover and topography and their interactions on  $\theta$  vertical and lateral patterns were examined.  $\theta$  was monitored on a very detailed time scale for 18 months in three hillslope positions allowing a high resolution analysis essential to understand spatial and temporal variations in  $\theta$  and therefore, offering new and important information concerning  $\theta$  in a Mediterranean karst environment.

## STUDY AREA AND METHODS

### Site description

The study was carried out at El Llano de los Juanes (Fig. 1), an experimental site located in the upper plateau of Sierra de Gádor (Almería, SE Spain), a mountain range reaching 2,242 m a.s.l. formed by thick series of Triassic limestone and highly permeable dolomites, fractured rocks with intercalated calc-schists of low permeability underlain by Permian impermeable metapelites (Gonzalez-Asensio et al., 2003; Li et al., 2007; Vandenschrick et al., 2002). The climate in Sierra de Gádor is on the boundary between Mediterranean semiarid and Mediterranean sub-humid climate, marked by the irregularity of rainfall. Rainfall and temperature strongly vary with altitude; 171 mm of mean annual rainfall and 17°C of mean annual temperature are recorded on the southern footslopes whereas about 600 mm of mean annual rainfall and 11°C are recorded at the summit (Vandenschrick et al., 2002). Current land use is low intensity grazing by sheep and goats.

The experimental area of “Llano de los Juanes”, about 2 km<sup>2</sup>, at 1,600 m a.s.l. is a relatively flat area (Fig. 1) corresponding to a well-developed karstic plateau (Li et al., 2007) fragmented and slightly tilted to the East. The climate is Mediterranean sub-humid. Average annual rainfall at “La Zarba” weather station (10.4 km from the field site) over a 30 year period has been 463 mm with a high inter-annual coefficient of variation (138.3%). The recorded rainfall intensities during the period studied in “El Llano de los Juanes” were, in general, quite low. The maximum  $I_{5min}$  was 78.1 mm h<sup>-1</sup> during one event, however only 12% of rainfall events higher than 1 mm had a maximum  $I_{5min}$  higher than 15 mm·h<sup>-1</sup>. Two main landforms can be distinguished in the study area: flat areas, which represent 76% of the total area, and hillslopes, 24%. Hillslopes are short, maximum 100 m long, with slope gradients ranging between 1° and 40°.

Rock outcrops are very frequent (Li et al., 2007) and soils are very thin (30–35 cm) and stony. The main soil unit was identified by Oyonarte (1992) as Lithic Haploxeroll - Lithic Ruptic Argixeroll complex. The main features of these soils are the high clay and organic matter contents (Oyonarte et al. (1994) reported organic matter content up to 8.8% in A<sub>h</sub> horizons in the site) and high infiltration capacities (Li et al., 2008). Vegetation is generally sparse and mainly consists of patchy, dwarf, perennial shrubs and grasses (50–60%) forming a mosaic with rock outcrops (10–15%) and bare soil, generally with abundant stones (25–30%) (Li et al., 2007). The woody shrubs are dominated by *Genista* while *Festuca* predominates in the herbaceous stratum.

The scientific interest of this area is enhanced by isotopic studies which have shown that the main recharge area to the deep aquifers of Campo de Dalías lies in this carbonated mountain, precisely in its central plateau, at altitudes between 1400 and 1800 m a.s.l. (Vallejos et al., 1997), where the study area is located.

### Methods

#### Soil water content and precipitation

Soil water content ( $\theta$ ) was measured using a capacitance sensor based on the Self-Balanced Impedance Bridge (SBIB) technique (Patent No. 9401681; Vidal, 1994; Vidal et al., 1996). Sensor output also included soil temperature and water dielectric-constant compensation. SBIB probes had been calibrated against TDR probes, gravimetric moisture measurements and laboratory experiments for a wide range of soil salinity

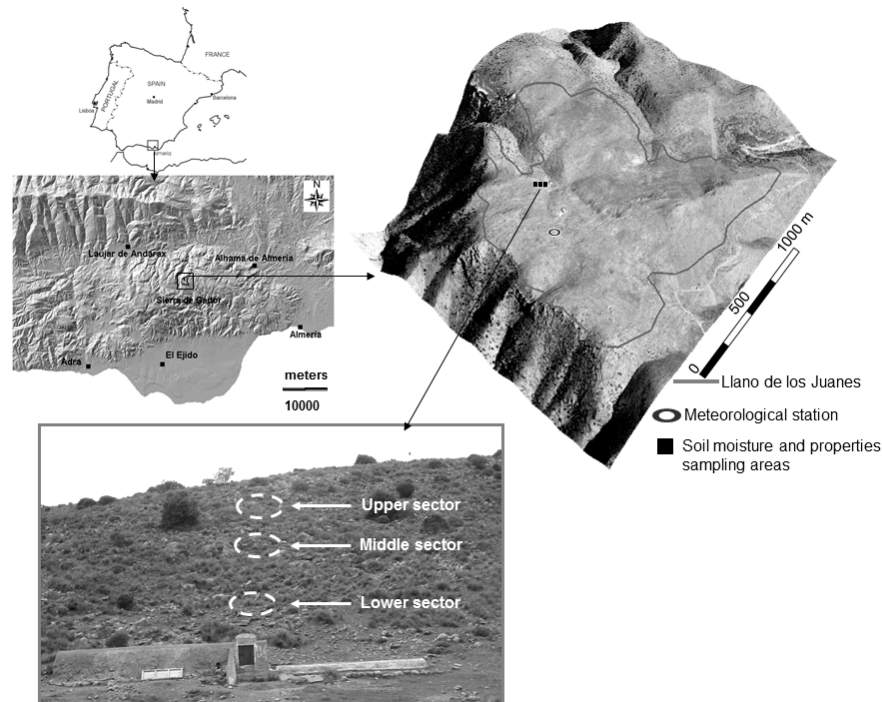


**Fig. 1.** Location of the study area. The location of soil moisture sampling and monitoring sites is marked on the map compiled from a DEM (10 m resolution) and on the hillslope photo.

levels and soil temperatures (Vidal et al., 1996) and successfully used to monitor  $\theta$  in several environments from SE Spain (Canton et al., 2004; Puigdefàbregas et al., 1998, 1999).  $\theta$  data were stored every 30 minutes in Campbell CR10X data loggers. To save energy from the batteries, the sensors were switched on during 3 minutes at 30-minute intervals,  $\theta$  was measured during the last 2 minutes and the averages were recorded.

A total of 18  $\theta$  probes were installed in a 95 m long, East facing hillslope with mean slope gradient of 25°. Probes were set under bare soil at three selected positions of the hillslope: upper, middle and lower sectors (Fig. 1). At each position two different depths were considered, 0.06 m and 0.25 m coinciding with the two soil horizons identified in the soil (A: 0–10 cm and Bt: 10–35 cm). It was not possible to install deeper probes in these shallow soils (about 0.35 m deep). Three sensors were installed in each position and depth (the three replicates were separated about 10 cm) and after the stabilization period of one month and a half,  $\theta$  was measured during 17 months. The data series is complete at the upper hillslope position, however, some problems arose at the middle and especially at the lowest hillslope positions due to incorrect functioning of some probes, battery discharges or dataloggers disconnections and robberies, that caused loss of data and several gaps in the data series, especially at 0.25m depth of the lowest position where only about four months of data are available. Fortunately, the measurement period included representative wet and dry cycles. The results refer to the average  $\theta$  measured at each position and depth. Daily  $\theta$  was calculated as the average of 30-min recordings. Also annual and seasonal  $\theta$  were calculated using the daily averages.

Rainfall amount and intensity were recorded by an automatic 0.20 mm-resolution tipping-bucket rain gauge (Davis, model 7852M). Based on daily volume the antecedent precipitation index (API) was estimated. API was calculated according to Fedora and Beschta (1989), and considering a period of 7 days (Eq. 1),

$$API = \sum_{t=7}^{t=1} P_t K^t \quad (1)$$

where  $API$  is the antecedent precipitation index ( $\text{mm d}^{-1}$ ),  $P$  is the precipitation (mm) in day  $t$ , and  $K$  is the dimensionless recession coefficient.  $K$  was fixed to 0.94, based on previous studies in semiarid areas (Polyakov et al., 2010).

#### *Soil properties, soil surface cover and topography*

To analyse the effect of static factors on  $\theta$ , soil properties and topography were analysed on the positions where  $\theta$  was monitored. Although this paper does not aim to analyse the influence of soil surface components (i.e. plants, bare soil, stones etc.) on  $\theta$ , because all probes were installed under bare soil, soil cover of the surrounded area can affect  $\theta$  at the sampling area, soil cover was also estimated for each  $\theta$  sampling location.

Composite soil samples (obtained by mixing four subsamples) collected near probe locations were used for the following soil analyses: i) particle size distribution by classical sieving methods for gravel and sand and by Robinson's pipette for silt and clay fractions after removal of organic matter (Gee and Bauder, 1986); ii) water retention at  $-33$  kPa and  $-1500$  kPa by pressure plates; available water capacity (AWC) was calculated as the difference in water content at tensions of  $-33$  kPa and  $-1500$  kPa considering the available water provided by gravel (Oyonarte et al., 1997); iii) organic matter content using the Walkley-Black wet digestion method (Nelson and Sommers, 1982) and iv) bulk density by the excavation method (Blake and Hartge, 1986).

Soil cover was estimated for each  $\theta$  sampling location in 3 x 3 m plots using a 0.5 m x 0.5 m rigid square metal frame with a 10 cm screen. Three random 1 x 1 m squares were sampled in each 3 x 3 m plot. Cover values were measured for perennial and annual plants, bare soil (crusted and non-crusted), litter and stones (embedded or not embedded) distinguishing by size

(<7.5cm; between 7.5 cm and 25 cm; >25 cm). Terrain attributes (slope gradient and aspect and potential contributing area) were extracted for the different positions where  $\theta$  was monitored, using a Digital Elevation Model (5-m resolution), using Idrisi Taiga software (Idrisi GIS Taiga, Clark Labs, Clark University: Worcester, MA, USA, 2012). For the potential contributing area the software uses a modification of the algorithm described by Jenon and Domingue (1988).

Differences in  $\theta$  between different hillslope positions and depths were analysed using general linear models (GLM). More precisely, we used hillslope position and depth as categorical predictors, whereas API index was considered as a continuous predictor. P values lower than 0.05 were interpreted as significant effects, and residuals were visually scrutinized and did not deviate substantially from normal. The analysis was done using in STATISTICA 8.0 (StatSoft, Inc., Tulsa, Oklahoma, USA).

## RESULTS

### Topography, cover and soil properties heterogeneity along the hillslope

Surface cover and topography showed marked differences between hillslope positions (Table 1). The highest plant cover was observed in the upper part of the hillslope (45%), and decreased downslope, despite slope decreased and potential contributing areas increased. Stone cover, on the other hand, increased from values around 35%, on the upper sector of the hillslope, to 55% on the lower sector. However, rock outcrops appeared upslope the  $\theta$  monitoring area located in the upper sector of the hillslope, but not in the other sectors. Soil properties also showed contrasting differences among hillslope positions and also between depths (Table 2). In general, clay content of both A and Bt horizons increased downslope, whereas silt content showed the opposite pattern. Sand content was higher in the A horizon than in the Bt at the upper and lower sectors, with the highest values on the upper part (19.8%). The middle sector, on the other hand, showed higher sand in the Bt horizon than in the A, with values of 9.1% and 14.8% respectively.

As results of the differences in soil properties, contrasting differences in both infiltration capacity and Ks were observed in the different hillslope positions. The upper sector showed the highest infiltration rate with about  $54 \text{ mm}\cdot\text{h}^{-1}$ . Ks was also higher on this sector when compared with the middle and lower ones, especially at lower tension, and both, infiltration capacity and Ks, decreased downslope (Table 2). Available water showed the same pattern, with decreasing values from the upper sector to the lower one, at both soil depths.

### Differences in $\theta$ among hillslope positions and depths

As expected, on the studied hillslope  $\theta$  significantly increased with the API index (Table 3). Hillslope position and depth also exerted a significant effect on  $\theta$  (Table 3). However, depth effect on  $\theta$  varied among hillslope positions, as reflected by the significant interaction between the two factors (Table 3). Thus, contrasting differences in  $\theta$  were observed among hillslope positions at the different depths (Figure 2 and 3).

When the response of the different hillslope sectors and depth are analysed more in detail, we also observed different behaviours depending on the study period. Figure 2 shows the evolution of  $\theta$  at the three studied hillslope positions (upper, middle and lower sectors) at 0.06 m and 0.25 m depths (Figs. 2a and 2b, respectively). As a general trend,  $\theta$  increased with

**Table 1.** Site characteristics (ground cover and terrain attributes) at the three studied positions on the hillslope.

Site characteristics	Positions in hillslope		
	Upper	Middle	Lower
Plant cover (%)	45	44.5	14.5
Stone cover (%)	36	30.5	55
Surface crusts (%)	10	5	2
Bare soil (%)	6	19.5	22
Litter (%)	3	0.5	6.5
Slope gradient (°)	35.4	28.6	19.8
Slope aspect (°)	295	295	295
Potential Contributing area (m <sup>2</sup> )	10	200	700

**Table 2.** Soil properties at the three studied positions on the hillslope and at two depths.

$K_{unsat}$ : Unsaturated hydraulic conductivity. \*: The infiltration rates correspond to rainfall simulations (constant rainfall intensity:  $55 \text{ mm}\cdot\text{h}^{-1}$ ) under dry conditions during 1 hour.  $K_{unsat}$  and infiltration rates were obtained from the experiments performed by Li et al. (2008) and Li et al. (2011).

Soil Properties	Depth (cm)	Positions at the hillslope		
		Upper	Middle	Lower
Clay (%)	0–10	21.4	47.8	55.4
	10–35	52.9	60.4	68.1
Silt (%)	0–10	58.8	43.2	32.5
	10–35	34.5	24.8	21.6
Sand (%)	0–10	19.8	9.1	12.1
	10–35	12.6	14.8	10.3
Organic matter (%)	0–10	7.3	7.2	3.8
	10–35	6.3	5.2	1.3
Available water (mm)	0–10	10.44	6.52	7.70
	10–35	17.95	15.56	18.75
Bulk density (g·cm <sup>-3</sup> )	0–15	1.1	1.0	1.2
Infiltration (mm·h <sup>-1</sup> )*		53.9	50.9	44.0
Tensions (cm)				
$K_{unsat}$ (mm·h <sup>-1</sup> )	3cm	69.7	19.9	3.8
	6cm	2.4	1.93	1
	12cm	0.3	0.4	0.4

**Table 3.** Summary of General Linear Model (GLM) for  $\theta$ , antecedent precipitation index (API), hillslope position and depth.

	F	p	Partial eta-squared
Intercept	9864.182	0.00	0.818728
API	523.583	0.00	0.193377
Hillslope position	557.887	0.00	0.338137
Depth	112.548	0.00	0.049007
Interaction position-depth	91.813	0.00	0.077557

depth, with higher  $\theta$  at 0.25 m depth than at 0.06 m. Moreover, at 0.25 m soil depth,  $\theta$  clearly increased downslope along the entire study period, with daily values at the lower position that varied from 15%, on the dry period, to more than 45 % during the wettest season (Fig 2b). However, at 0.06 m depth  $\theta$  was higher in wet periods at the upper position than at the middle one and in some cases than at lower ones, with maximum daily values close to 33% (Fig 2a). During dry periods, on the other hand,  $\theta$  at 0.06 m depth showed similar patterns to  $\theta$  at 0.25 m depth, with  $\theta$  increasing from the upper to the lower position ( $\theta$  about 2% and 7.5% for summer, respectively). These differences were more evident at event scale as showed in Fig. 3.

After a rainfall of 5.3 mm with a maximum intensity of  $24.4 \text{ mm}\cdot\text{h}^{-1}$  in 3 minutes occurred on July, Fig 3a shows an increase in daily  $\theta$  at the upper hillslope and no change on daily  $\theta$  at 0.06 m depth at the middle slope. In Fig. 3b the  $\theta$  increase

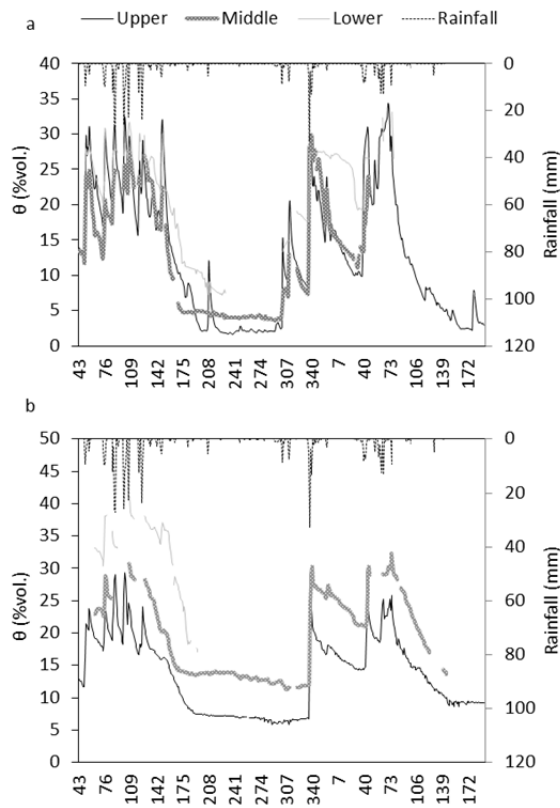


**Fig. 2.** Evolution of rainfall and daily mean  $\theta$  at 0.06 m (a) and 0.25 m depth (b) at the three studied slope positions.

is much higher at 0.06 m in the upper sector than in the middle sector under a rainfall of 7.72 mm and  $I_{3min}$  of 40.6 mm h<sup>-1</sup>.

Moreover, it can be observed that the increase in  $\theta$  at 0.06 m was faster at the upper sector, whereas more time was necessary to reach the maximum  $\theta$  at the middle one. For larger rainfall event (Fig. 4) and using 30-minute resolution data, it can be observed greater and faster increases in  $\theta$  and losses of water during dryings at the surface layer in the upper position respect the other positions and depths. Also at middle and lowest positions  $\theta$  maintained high values during longer periods.

Thus, for the days showed in Fig. 4, at the middle position at 0.25 cm depth,  $\theta$  surpassed the water content at field capacity for this soil during 37.5 hours.

## DISCUSSION

### Interrelated effects of “static” factors on $\theta$ lateral patterns

$\theta$  differences among hillslope positions and depths were motivated by the spatial heterogeneity (lateral and vertical) of soil properties, ground cover and topography along the hillslope as shown in Tables 1 and 2. Whereas the upper horizon of the upper hillslope sector showed high sand contents, clay content is higher in the subsurface horizon and increases downslope at both soil depths (Table 2), probably as the result of both clay transport by overland flow (this mechanism has been described by other authors, i.e. Cerdà (2002), in Mediterranean environments), and/or clay illuviation, also a well-known process in these environments (Ceballos et al., 2002; Cerdà, 2002; Gicheru et al., 2004; Philips, 2004; Yaalon, 1997). In fact, Delgado et al. (2003) described Bt horizons in soils belonging to the same soil unit in a nearby area to the study site. In the studied

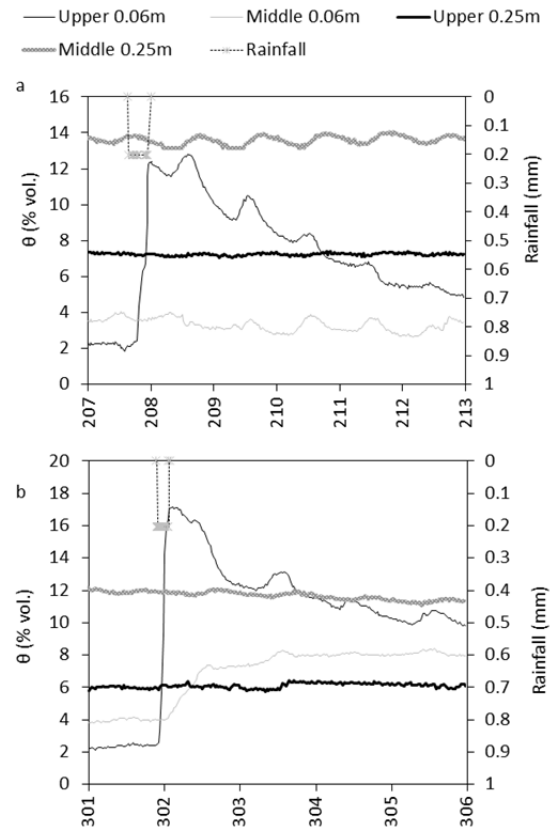


**Fig. 3.** Different behaviour of  $\theta$  (30 minute intervals) evolution at 0.06 m and 0.25 m depth in the upper and middle hillslope sectors after two rainfall events: DOI 209 (3a) and DOI 302 (3b).

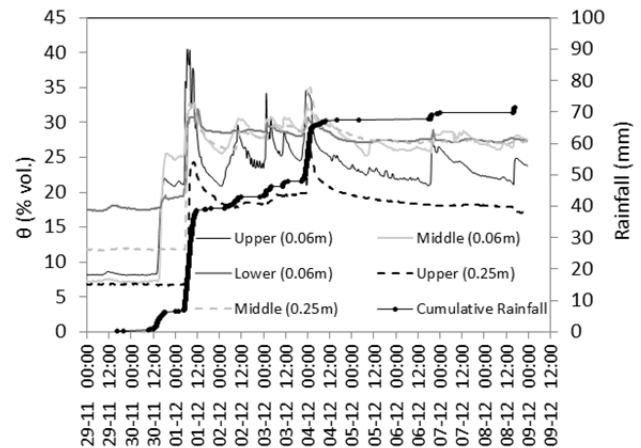


**Fig. 4.** Evolution of rainfall and 30 minutes-resolution  $\theta$  at 0.06 m and 0.25 m depths at the three studied slope positions during a wet period. At the lowest position  $\theta$  at 0.25 m depth was not available for these days.

hillslope, it would be expected that the increase of clay and the lower sand contents downslope at 0.06 m soil depth (Table 2) which also would go along with a higher potential contributing area, would result in higher  $\theta$  values at downslope position. However, the upper sector of the hillslope showed higher unsaturated hydraulic conductivity ( $K_{unsat}$ ) for the surface horizon and infiltration rates (Table 2). Differences in both,  $K_{unsat}$  and infiltration rates, have also been reported by Li et al. (2008) in the site, and may promote higher and faster water infiltration into the upper soil horizon than in others hillslope positions

especially after small rainfall events (Figure 2a), increasing  $\theta$  at the surface horizon at this position. Looking at a more detailed temporal scale (Figure 4) it can be appreciated the higher  $\theta$  increases during rainfalls at the surface horizon at the upper position, but also the faster loss of water after the rainfall.

Other factors like the higher plant cover (Table 1), which must be reinforced by the higher available water for plants at the upper position, the greater soil organic matter content (see Table 2) and the presence of rock outcrops upslope the  $\theta$  monitoring area of the upper hillslope sector also contribute to this  $\theta$  pattern, and stresses the important role that the interaction of other factors plays on the  $\theta$  spatial pattern, modifying the expected influence of soil texture and contributing area. Moreover, the increase of potential contributing area downslope cannot be strictly applied to a karstic hillslope where the frequency and magnitude of runoff generation are low and where deep cracks are responsible for surface runoff discontinuities over short distances and because runoff hardly travel several meters as a continuous flow. Under these conditions the effective contributing area is controlled by the spatial distribution of runoff sources and sinks, like cracks or rock outcrops, respectively. In the study area, Li et al. (2007) reported the higher presence of rock outcrops at the upper sectors of hillslopes than in the middle and bottom ones. In our case, a rock outcrop about 1 m<sup>2</sup> was located just upslope the upper sector monitoring area. These rocks outcrops function as runoff sources supplying extra water, even during low magnitude and low intensity events (Figure 3), to the immediately downslope soils and contributing to the wetter regime in the upper hillslope sector at 0.06 m during rainy periods (Fig. 2a). During rainfall periods in which the hydrological connectivity along the hillslope is not reached, this extra water supply in the upper sectors would contribute to explain the higher  $\theta$  contents found at the soil surface layers (0.06 m) in contrast to the lower values measured at the middle and bottom sectors. This statement is supported by Figure 3, and also by Li et al. (2011), who measured very high runoff coefficients between 71% (under dry conditions) and 83% (under wet conditions) on rock outcrops under quite intense simulated rainfall. Other factors that have been reported to influence moisture differences among hillslope positions, such as hydrological rain (Kidron et al., 2009) or evaporation (Kidron and Zohar, 2010) probably could not explain the showed patterns because slope gradient at the upper hillslope position is higher than at the other positions (see Table 1) and it would be expected lower rain amounts at the upper position. In addition aspect is the same for the three positions. During dry periods, e.g. summer, direct rainfall infiltration and run-on contribution from upslope rock outcrops are insignificant explaining the driest regime at 0.06 m at the upper hillslope sector.

At 0.25 m, the wettest  $\theta$  regime appears at the lowest hillslope position at 0.25 m soil depth (Figure 2b). The higher soil clay content downslope, especially at this depth (Table 2), and its effect on water retention, could explain this pattern (Jawson and Niemann, 2007). At the upper position, the relatively lower  $\theta$  at 0.25m could be attributed to the contrasting properties between surface and subsurface soil horizons. Thus, the uppermost soil layer, with a silty loam texture, showed high  $K_{unsat}$  under low tensions (Table 2), which may reflect rapid infiltration by macropores. However, at depth, under the occurrence of a clayey subsurface layer (horizon Bt), lower infiltration rates and  $K_{unsat}$  are expected, especially at lower tensions. These differences in infiltration capacities, along with the steeper slope gradient at the upper sector (see Tables 1 and 2), would allow saturation of the uppermost soil layer and a water

excess at the boundary layer between uppermost soil and subsurface layers (i.e. A and Bt horizons). This excess of water may be intercepted by cracks and fissures allowing the infiltration of water and acting as a possible recharge water, or may be received, at least partially, by soils downslope, increasing their soil moisture (Figure 2b). At the middle and lowest positions of the hillslope,  $\theta$  at 0.25 m remains saturated for extended time (see above the example for the middle position in Fig. 4), and may also be contributing to groundwater recharge through fissure and cracks.

### Interrelated effects of soil properties on $\theta$ vertical patterns

The increases in  $\theta$  after a rainfall event were most obvious in upper soil layers and were dampened with depth as other authors have described (English et al., 2005; Tromp-Van Meerveld and McDonnell, 2006). As expected, for the medium and lower part of the hillslope,  $\theta$  is higher at 0.25 m than at 0.06 m throughout the entire period. Apart from the effect of the higher vapour pressure deficit on surface layer respect deeper layers, the soil dries out more slowly at 0.25 m due to the higher clay content found in the subsurface horizon (Table 2) that increases water retention and reduce evaporation losses as in other clay-rich soils of semiarid environments (English et al., 2005). For the upper position, as Fig. 5 shows,  $\theta$  is higher at 0.25 m only under dry conditions (in summer or when  $\theta$  decreases under about 15%). The rest of the time, storms of small to medium magnitude provoked runoff yield at the upslope rock outcrops in this sector and this additional water together with the rainfall wetted the upper soil layers. However, the important increase in clay content and a reduction in sand from the upper horizon to the deeper one, at this position (Table 2), may result in a reduction of infiltration capacity and in a less permeable layer in depth. As we explained above, this could promote an excess of water flowing downslope which might contribute to increase downslope  $\theta$  at 0.25 m and explain the higher  $\theta$  at 0.06 m in respect of 0.25 m at this position, especially in autumn and winter when evapotranspiration is reduced. Moreover, the soil water content at 0.25 m at both  $-33$  kPa (32.3% vol.) and saturation (55.6% vol.) was substantially lower than  $\theta$  at 0.06 m (39.6% vol. and 66.2% vol., respectively), while the soil water content at  $-1.5$  MPa was very similar at both soil depths.

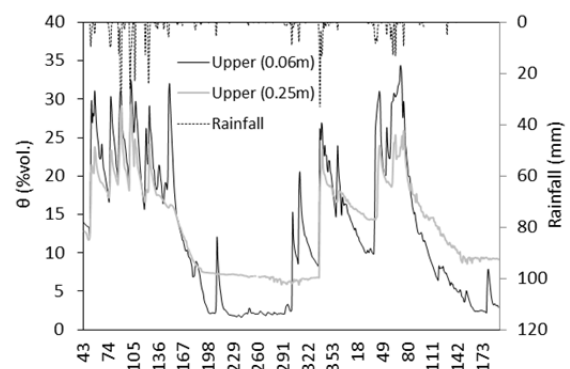
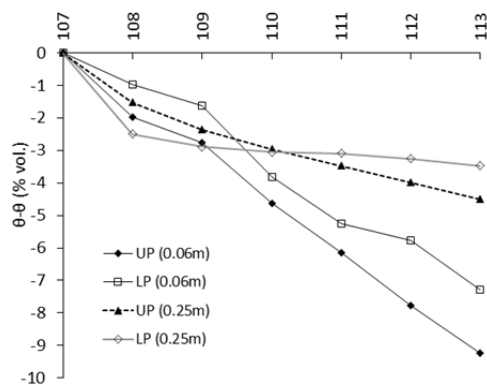


Fig. 5. Evolution of rainfall and daily mean  $\theta$  at two depths (0.06 m and 0.25 m) at the upper hillslope.

When the drying down periods after different rainfall events were analysed at more detailed scale (an example is shown in Fig. 6), it was observed that, in general, the water depletion rate decreased downslope at both depths and  $\theta$  decreased more rapidly at shallow horizons because of the lower clay contents

and the higher impact of evaporation losses. This pattern reveals that differences in water depletion rate are strongly governed by soil texture under similar climatic conditions, supporting that the spatial variability of  $\theta$  in inter-storm periods is closely related to soil texture (Yoo et al., 1998). However, after some rainy periods deviations to this pattern were observed, for example the rainfall that occurred on the day of the year 106: the first day after the rainfall, we observed the fastest water depletion at 0.25 m depth on the lowest position (Fig. 6). Later, after the first day, this is the position where the soil dried more slowly (Fig. 6),  $\theta$  changing from 38.6% to 37.6 % in 5 days. At this position and depth, just after the rainfall,  $\theta$  reached a peak value of 44% exceeding the field capacity threshold measured at the laboratory (35.3% vol). This results in deep drainage losses and explains the rapid water depletion the first day after the rainfall event. Evaporation losses may also contribute to this process, especially in the following days, when depletion rate is much lower. However they are, in general, quite low due to the extensive stone cover in the lower sector of the hillslope (Table 1). In the other positions  $\theta$  only exceeded field capacity for 9 hours at 0.25 m depth in the upper sector of the hillslope but the losses from drainage were not so evident at a daily scale.



**Fig. 6.** Depletion of  $\theta$  at the upper hillslope (UP) and lower hillslope (LP) sectors with regard to initial soil moisture conditions ( $\theta_0$ ) at 0.06 m and 0.25 m soil depth after a rainfall event.

## SUMMARY AND CONCLUSIONS

The evolution of  $\theta$  in Llano de los Juanes during a long period shows that “static” factors play an important role on  $\theta$  spatial distribution during both dry and wet states. A strong variability depending on the position at the hillslope was found. At 0.25 m soil depth,  $\theta$  always increases downslope, with soil clay content as the main controlling factor. However, the pattern of  $\theta$  in the surface horizon along the hillslope coincides with that found in subsurface horizon only during dry periods, when the main controlling factor is also the clay content increasing downslope. During wet periods, the wettest regime at the surface horizon is found in the upper hillslope sector. At this position, the highest infiltration capacity and  $K_s$ , together with the presence of rock outcrops upslope the sampling area acting as runoff sources contributes to explain the differences in the soil surface layers with regards the middle and lower sectors. Their effect is enhanced because, for most rainfall events, the hillslope is not hydrologically connected and runoff generation is restricted to both rock outcrops (more frequent in the upper hillslope sector) and bare soil in the lower slope sector when subsurface layers (very rich in clay) become saturated.

Moreover, surface infiltration capacity,  $K_{unsat}$  and rock outcrops also affect the vertical  $\theta$  patterns, in such a way that in

the upper hillslope sector,  $\theta$  was higher at 0.25 m depth only during dry periods, while for wet periods the influence of rock outcrops upslope supplying extra water to the immediately downslope soils causes the shallow soil layers to have higher  $\theta$  than the deeper ones. For the middle and lowest hillslope sectors  $\theta$  was lower at 0.06 m than at 0.25 m throughout the entire period studied because  $\theta$  depletion is faster in upper soil layers due to the substantial lower clay content in relation to subsurface layers. The results have shown the important role that soil texture, rock fragment distribution and cracks and fissures plays as a runoff sources in the hillslope system, not only in arid and semiarid systems, but also in Mediterranean sub-humid environments. The influence of these factors and their interactions leads to vertical and horizontal  $\theta$  patterns along the hillslope, which are different than expected due to topography. They can also affect the relationships, as stated in previous works, between observed  $\theta$  and some soil properties or topographic attributes as indicators of near surface  $\theta$ . Furthermore, spatially distributed hydrologic models that predict  $\theta$  patterns as well as other components of the water balance should be parameterized taking into account all these factors and their interactions in Mediterranean environments, with especial attention to rock outcrops. However, these relationships are more complicated in karstic areas, where the effect and cracks and fissures on deep infiltration difficult their analysis. Thus more studies in these environments are recommended in order to produce more general conclusions and to allow their inclusion in hydrological models. Moreover, it is necessary to analyse the effect of the interactions among “static” factors like soil properties, cover and topography, and “dynamic” factors like precipitation, evaporation or runoff generation on  $\theta$ , at temporal detailed scales, especially in systems with accentuated spatial-temporal variability like Mediterranean karstic areas.

**Acknowledgements.** This work was funded by the Spanish National Plan for Research, Development and Innovation and including European Union of Regional Development Funds, under the BACARCOS (CGL2011-29429), RESUCI (CGL2014-59946-R) and CARBORAD (CGL2011-27493) research projects. The authors would like to thank Alfredo Durán Sánchez and Diego Moreno for their invaluable help in the field work and Daniel Larue for correcting and improving the English text.

## REFERENCES

- Albertson, J.D., Montaldo, N., 2003. Temporal dynamics of soil moisture variability: 1. Theoretical basis. *Water Resour. Res.*, 39, 10: SWC21-SWC214.
- Benoit, G., Comeau, A., 2005. A sustainable future for the Mediterranean: the Blue Plan’s environment and development outlook. Earthscan, London.
- Blake, G.R., Hartge, K.H., 1986. Bulk Density. In: Klute, A. (Ed.): *Methods of Soil Analysis, Part I. Physical and Mineralogical Methods*. Agronomy Monograph no. 9 (2nd ed.), American Society of Agronomy, Madison, WI, pp. 363–375.
- Calvo-Cases, A., Boix-Fayos, C., Imeson, A.C., 2003. Runoff generation, sediment movement and soil water behaviour on calcareous (limestone) slopes of some Mediterranean environments in southeast Spain. *Geomorphology*, 50, 1–3, 269–291.
- Cammeraat, L.H., 2004. Scale dependent thresholds in hydrological and erosion response of a semi-arid catchment in southeast Spain. *Agr. Ecosyst. Environ.*, 104, 317–332.

- Campra, P., García, M., Canton, Y., Palacios-Orueta, A., 2008. Surface temperature cooling trends and negative radiative forcing due to land use change towards greenhouse farming in southeastern Spain. *J. Geophys. Res. - Atm.*, 113, D18109, doi: 10.1029/2008JD009912.
- Canton, Y., Domingo, F., Solé-Benet, A., Puigdefàbregas, J., 2001. Hydrological and erosion response of a badlands system in semi-arid SE Spain. *J. Hydrol.*, 252, 65–84.
- Cantón, Y., Solé-Benet, A., Domingo, F., 2004. Temporal and spatial patterns of soil moisture in semiarid badlands of SE Spain. *J. Hydrol.*, 285, 1–4, 199–214.
- Canton, Y., Solé-Benet, A., de Vente, J., Boix-Fayos, C., Calvo-Cases, A., Asensio, C. et al., 2011. A review of runoff generation and soil erosion across scales in semiarid south-eastern Spain. *J. Arid Environ.*, 75, 1254–1261.
- Castro, J.A., Martín-Lopez, B., Lopez, E., Plieninger, T., Alcaraz-Segura, D., Vaughn, C.C., Cabello, C., 2015. Do protected areas networks ensure the supply of ecosystem services? Spatial patterns of two nature reserve systems in semi-arid Spain. *Appl Geogr.*, 60, 1–9.
- Ceballos, A., Martínez-Fernández, J., Santos, F., Alonso, P., 2002. Soil-water behaviour of sandy soils under semi-arid conditions in the Duero Basin (Spain). *J. Arid Environ.*, 51, 501–519.
- Cerdà, A., 1997. Seasonal changes of the infiltration rates in Mediterranean scrubland on limestone. *J. Hydrol.*, 198, 209–225.
- Cerdà, A., 2002. The effects of season and parent material on water erosion on highly eroded soils in eastern Spain. *J. Arid Environ.*, 52, 319–337.
- Chamizo, S., Canton, Y., Lázaro, R., Domingo, F., 2013. The role of biological soil crusts in soil moisture dynamics in two semiarid ecosystems with contrasting soil textures. *J. Hydrol.*, 489, 74–84.
- Dehotin, J., Breil, P., Braud, I., de Lavenne, A., Lagouy, M., Sarrazin, B., 2015. Detecting surface runoff location in a small catchment using distributed and simple observation method. *J. Hydrol.*, 525, 113–129.
- Delgado, R., Martín-García, J.M., Oyonarte, C., Delgado, G., 2003. Génesis of the *terrae rossae* of the Sierra de Gádor (Andalusia, Spain). *Eur. J. Soil Sci.*, 54, 1–16.
- Eilers, V.H.M., Carter, R.C., Rushton, K.R., 2007. A single layer soil water balance model for estimating deep drainage (potential recharge): An application to cropped land in semi-arid North-east Nigeria. *Geoderma*, 140, 1–2, 119–131.
- English, N.B., Weltzin, J.F., Fravolini, A., Thomas, L., Williams, D.G., 2005. The influence of soil texture and vegetation on soil moisture under rainout shelters in a semi-desert grassland. *J. Arid Environ.*, 63, 324–343.
- Entekhabi, D., Rodríguez-Iturbe, I. and Castelli, F., 1996. Mutual interaction of soil moisture state and atmospheric processes. *J. Hydrol.*, 184, 3–17.
- Entin, J.K., Robock, A., Vinnikov, K.Y., Hollinger, S.E., Liu, S.X., Namkhai, A., 2000. Temporal and spatial scales of observed soil moisture variations in the extratropics. *J. Geophys. Res.*, 105(D9), 11865–11877.
- Famiglietti, J.S., Rudnicki, J.W., Rodell, M., 1998. Variability in surface moisture content along a hillslope transect: Rattlesnake Hill, Texas. *J. Hydrol.*, 210, 1–4, 259–281.
- Fedora, M.A., Beschta, R.L., 1989. Storm runoff simulation using an antecedent precipitation index (API) model. *J. Hydrol.*, 112, 121–133.
- Gee, G.W., Bauder, J.W., 1986. Particle-size analysis. In: Klute, A. (Ed.): *Methods of Soil Analysis*, part I. Physical and Mineralogical Methods, (2nd ed.). Agronomy 9. American Society of Agronomy, Madison, WI, pp. 383–411.
- Gicheru, P., Gachene, C., Mbuvi, J., Marea, E., 2004. Effects of soil management practices and tillage systems on surface soil water conservation and crust formation on a sandy loam in semi-arid Kenya. *Soil Till. Res.*, 75, 173–184.
- Gish, T.J., Walthall, C.L., Daughtry, C.S.T., Kung, K.-J.S., 2005. Landscape and watershed processes: Using soil moisture and spatial yield patterns to identify subsurface flow pathways. *J. Environ. Qual.*, 34, 1, 274–286.
- Gomez-Plaza, A., Martínez-Mena, M., Albadalejo, J., Castillo, V.M., 2001. Factors regulating spatial distribution of soil water content in small semiarid catchments. *J. Hydrol.*, 253, 211–226.
- Gonzalez-Asensio, A., Domínguez, P., Franqueza, P.A., 2003. Sistema costero de Sierra de Gádor. Observaciones sobre su funcionamiento y relaciones con los ríos Adra y Andarax, y con el Mar. In: López-Geta, J.A., de la Orden, J.A., Gómez, J.D., Ramos, G., Mejías, M., Rodríguez, L. (Eds.): *Coastal aquifers intrusion technology: Mediterranean countries (TIAC'03)*. IGME, Madrid, pp. 423–432.
- Grayson, R.B., Western, A.W., Walker, J.P., Kandel, D.D., Costelloe, J.F., Wilson, D.J., 2006. Controls on patterns of soil moisture in arid and semi-arid systems. In: D'Orico, P., Porporato, A. (Eds.): *Dryland Ecohydrology*. Springer, The Netherlands, pp. 109–128.
- Hébrard, O., Voltz, M., Andrieux, P., Moussa, R., 2006. Spatio-temporal distribution of soil surface moisture in a heterogeneously farmed Mediterranean catchment. *J. Hydrol.*, 329, 110–121.
- Jawson, S.D., Niemann, J.D., 2007. Spatial patterns from EOF analysis of soil moisture at a large scale and their dependence on soil, land-use, and topographic properties. *Adv. Water Resour.*, 30, 3, 366–381.
- Jenson, S., Domingue, J., 1988. Extracting topographic structure from digital elevation data for geographic information system analysis. *Photogramm Eng. Rem. S.*, 54, 11, 1593–1600.
- Jia, X., Shao, M., Wei, X., Wang Y., 2013. Hillslope scale temporal stability of soil water storage in diverse soil layers. *J. Hydrol.*, 498, 254–264.
- Kidron, G.J., Zohar, M., 2010. Spatial evaporation patterns within a small drainage basin in the Negev Desert. *J. Hydrol.*, 380, 3–4, 376–385.
- Kidron, G.J., Vonshak, A., Abeliovich, A., 2009. Microbiotic crusts as biomarkers for surface stability and wetness duration in the Negev Desert. *Earth Surface Processes and Landforms*, 34, 1594–1604.
- Koster, R.D., Dirmeyer, P.A., Guo, Z., Bonan, G., Chan, E., Cox, P., 2004. Gordon, C.T., 2004. Regions of Strong Coupling between Soil Moisture and precipitation, *Science*, 305, 5687, 1138–1140.
- Li, X.Y., Contreras, S., Solé-Benet, A., 2008. Unsaturated hydraulic conductivity in limestone dolines: Influence of vegetation and rock fragments. *Geoderma*, 145, 288–294.
- Li, X.Y., Contreras, S., Solé-Benet, A., Canton, Y., Domingo, F., Lázaro, R., Lin, H., Van Wesemael, B., Puigdefàbregas, J., 2011. Controls of non-uniform infiltration-runoff processes in a mountainous dry Mediterranean shrubland. *Catena*, 86, 98–109.
- Li, X.-Y., Contreras, S., Solé-Benet, A., 2007. Spatial distribution of rock fragments in dolines: A case study in a semiarid Mediterranean mountain-range (Sierra de Gádor, SE Spain). *Catena*, 70, 3, 366–374.
- Ludwig, J.A., Wilcox, B.P., Breshears, D.D., Tongway, D.J., Imeson, A.C., 2005. Vegetation patches and runoff-erosion as interacting ecohydrological processes in semiarid landscapes. *Ecology*, 86, 288–297.

- Martínez-Fernández, J., Ceballos, A., 2003. Temporal stability soil moisture in a large-field experiment in Spain. *Soil Sci. Soc. Am. J.*, 67, 1647–1656.
- Mayor, A.G., Bautista, S., Small, E.E., Dixon, M., Bellot, J., 2008. Measurement of the connectivity of runoff source areas as determined by vegetation pattern and topography: A tool for assessing potential water and soil losses in drylands. *Water Resour. Res.*, 44, Art. No. W10423
- Nelson, D.W., Sommers, L.E., 1982. Total carbon, organic carbon, and organic matter. In: Page, L.A., Miller, R.H., Kenney, D.R. (Eds.): *Methods of Soil Analysis. Part 2. Chemical and Microbiological Methods*, 2nd ed. American Society of Agronomy, Madison, WI, pp. 539–579.
- Oyonarte, C., 1992. Estudio edáfico de la Sierra de Gádor (Almería). Evaluación para usos forestales. Memoria de Tesis Doctoral, Depto. de Edafología y Química Agrícola, Universidad de Granada.
- Oyonarte, C., Pérez-Pujalte, A., Delgado, G., Delgado, R., Almendros, A., 1994. Factors affecting soil organic matter turnover in a Mediterranean ecosystems from Sierra de Gádor (Spain): an analytical approach. *Commun. Soil. Sci. Plant. Anal.*, 25, 11–12, 1929–1945.
- Oyonarte, C., Escoriza, I., Delgado, R., Pinto, V., Delgado, G., 1997. Water-retention capacity in fine earth and gravel fractions of semiarid Mediterranean mountain soils. *Arid Soil Res. Rehab.*, 12, 29–45.
- Penna, D., Brocca, L., Borga, M., Dalla-Fontana, G., 2013. Soil moisture temporal stability at different depths on two alpine hillslopes during wet and dry periods. *J. Hydrol.*, 477, 55–71.
- Philip, J.D., 2004. Geogenesis, pedogenesis, and multiple causality in the formation of texture-contrast soils. *Catena*, 58, 3, 275–295.
- Polyakov, V.O., Nearing, M.A., Nichols, M.H., Scott, R.L., Stone, J.J., McClaran, M.P., 2010. Long-term runoff and sediment yields from small semiarid watersheds in southern Arizona. *Water Resour. Res.*, 46, W09512, doi: 10.1029/2009WR009001.
- Puigdefábregas, J., 2005. The role of vegetation patterns in structuring runoff and sediment fluxes in drylands. *Earth Surf. Proc. Landf.*, 30, 133–147.
- Puigdefábregas, J., Del Barrio, G., Boer, M.M., Gutiérrez, L., Solé, A., 1998. Differential responses of hillslope and channel elements to rainfall events in a semi-arid area. *Geomorphology*, 23, 2–4, 337–351.
- Puigdefábregas, J., Solé, A., Gutiérrez, L., Del Barrio, G., Boer, M., 1999. Scales and processes of water and sediment redistribution in drylands: results from the Rambla Honda field site in Southeast Spain. *Earth-Science Reviews*, 48, 39–70.
- Pulido-Bosch, A., Pulido-Lebouf, P., Molina, L., Vallejos, A., Martín-Rosales, W., 2000. Intensive agriculture, wetlands, quarries and water management. A case study (Campo de Dalías, SE Spain). *Environl. Geol.*, 40, 1–2, 163–168.
- Ries, F., Lange, L., Schmidt, S., Puhlmann, H., Sauter, M., 2015. Recharge estimation and soil moisture dynamics in a Mediterranean, semi-arid karst region. *Hydrol. Earth Syst. Sci.*, 19, 1439–1456.
- Rivera, D., Lillo, M., Granda, S., 2014. Representative locations from time series of soil water content using time stability and wavelet analysis. *Environmental Monit Assess.*, 186, 12, 9075–9087.
- Rodríguez-Caballero, E., Canton, Y., Lázaro, R., Solé-Benet, A., 2014. Cross-scale interactions and nonlinearities in the hydrological and erosive behavior of semiarid catchments: The role of biological soil crusts. *J. Hydrol.*, 517, 815–825.
- Rodríguez-Caballero, E., Canton, Y., Jetten, V., 2015. Biological soil crust effects must be included to accurately model infiltration and erosion in arid and semiarid systems. *Geomorphology*, 241, 331–342.
- Rodríguez-Iturbe, I., Porporato, A., 2004. *Ecohydrology of Water-Controlled Ecosystems: Soil Moisture and Plant Dynamics*. Cambridge Univ. Press, New York.
- Saxton, K.E., Rawls, W.J., Romberger, J.S., Papendick, R.I., 1986. Estimating generalized soil-water characteristics from texture. *Soil Sci. Soc. Am. J.*, 50, 4, 1031–1036.
- Tokumoto, I., Heilman, J.L., Schwinning, S., McInnes, K.J., Litvak, M.E., Morgan, C.L., Kamps, R.H., 2014. Small-scale variability in water storage and plant available water in shallow, rocky soils. *Plant Soil*, 385, 193–204.
- Tromp-van Meerveld, H.J., McDonnell, J.J., 2006. On the interrelations between topography, soil depth, soil moisture, transpiration rates and species distribution at the hillslope scale. *Adv. Water Resour.*, 29, 293–310.
- Vallejos, A., Pulido-Bosch, A., Marttn-Rosales, W., Calvache, M.L., 1997. Contribution of environmental isotopes to the understanding of complex hydrologic systems. A case study: Sierra de Gádor, SE Spain. *Earth Surf. Proc. Landf.*, 22, 12, 1157–1168.
- Vandenschrick, G., van Wesemael, B., Frot, E., Pulido-Bosch, A., Molina, L., Stievenard, M., Souchez, R., 2002. Using stable isotope analysis ( $\delta D$ – $\delta^{18}O$ ) to characterise the regional hydrology of the Sierra de Gádor, south east Spain. *J. Hydrol.*, 265, 43–55.
- Vidal, S., 1994. Sensor para la determinación simultánea en suelos de humedad y conductividad eléctrica. España. Patente 9401681.
- Vidal, S., Domene, M.A., Solé, A., Puigdefábregas, J., 1996. Desarrollo y calibración de un nuevo sensor de humedad del suelo. IV Simposio sobre el agua en Andalucía, pp. 101–109. ITGME, Madrid.
- Western, A.W., Zhou, S., Grayson, R.B., McMahon, T.A., Blöschl, G., Wilson, D.J., 2004. Spatial correlation of soil moisture in small catchments and its relation to dominant spatial hydrological processes. *J. Hydrol.*, 286, 113–134.
- Wilson, D.J., Western, A.W., Grayson, R.B., 2004. Identifying and quantifying sources of variability in temporal and spatial soil moisture observations. *Water Resour. Res.*, 40, 2, W025071–W02507110.
- Yaalon, D.H., 1997. Soils in the Mediterranean region: what makes them different. *Catena*, 28, 157–169.
- Yang, J., Chen, H., Nie, Y., Zhang, W., Wang, K., 2016. Spatial variability of shallow soil moisture and its stable isotope values on a karst hillslope. *Geoderma*, 264, 61–70.
- Yoo, C., Valdes, J.B., North, G.R., 1998. Evaluation of the impact of rainfall on soil moisture variability. *Adv. Water Resour.*, 21, 5, 375–384.
- Yoo, C., Kim, S.J., Valdes, J.B., 2005. Sensitivity of soil moisture field evolution to rainfall forcing. *Hydrol. Process.*, 19, 1855–1869.
- Zhang, W., Wang, K.L., Chen, H.S., He, X.Y., Zhang, J.G., 2012. Ancillary information improves kriging on soil organic carbon data for a typical karst peak cluster depression landscape. *J. Sci. Food Agric.*, 92, 5, 1094–1102.
- Zhao, P., Tang, X.Y., Zhao, P., Wang, C., Tang, J.L., 2013. Identifying the water source for subsurface flow with deuterium and oxygen-18 isotopes of soil water collected from tension lysimeters and cores. *J. Hydrol.*, 503, 1–10.

Received 7 January 2016

Accepted 16 May 2016